satisfied). This is as near to a 'singularity' as this simple toy can approach. The effect is nevertheless striking in practice.

H. K. Moffatt
Isaac Newton Institute for Mathematical Sciences, 20 Clarkson Road, Cambridge CB3 0EH, UK
e-mail: hkm2@newton.cam.ac.uk

1. Pars, L. A. *Treatise on Analytical Dynamics* (Heinemann, London, 1965).
2. Euler, L. *Theoria Motus Corporum Solidorum Seu Rigidorum* (Greifswald, 1765).

Molecular transistors

Potential modulations along carbon nanotubes

True molecular-scale transistors have been realized using semiconducting carbon nanotubes[1–5], but no direct measurements of the underlying electronic structure of these have been made. Here we use a new scanning-probe technique to investigate the potential profile of these devices. Surprisingly, we find that the potential does not vary in a smooth, monotonic way, but instead shows marked modulations with a typical period of about 40 nm. Our results have direct relevance for modelling this promising class of molecular devices.

The principle of our scanning-gate potential-imaging (SGPI) technique is as follows. An individual semiconducting single-wall carbon nanotube is connected to two metal electrodes, and this transistor is switched to a conducting state by a negative gate voltage, V_g (Fig. 1a). A current flows when a bias voltage, V_b, is applied. At a close distance above the device surface, we scan the tip of an atomic-force microscope (AFM), on which a positive tip voltage, V_t, is applied. The AFM tip acts as a local gate and induces a local potential barrier (Fig. 1b) when it is above the tube. This can reduce the hole current through the nanotube, which is recorded as a function of the tip position (Fig. 1c). The main point of SGPI is that the current reduction depends on the original local potential of the tube. In this way, SGPI maps out the local potential profile of the nanotube.

The top images in Fig. 1d,e show regular AFM images of two different samples with their corresponding SGPI measurements at different bias voltages underneath. The most remarkable feature of these images is that they show a sequence of current dips along the tubes. The dips appear to be confined to the region between the electrodes. Surprisingly, they are rather evenly spaced, with a distance of about 40 nm for the sample in Fig. 1d, and 36 nm for the sample in Fig. 1e. These observations indicate that the edge of the valence band does not vary in a smooth monotonic way. Instead, they point to a potential that is significantly modulated, creating a sequence of barriers for the hole carriers (Fig. 1b). Similar SGPI measurements on metallic tubes did not show any contrast.

The effect of increased bias voltage is illustrated in the lower panels of Fig. 1d,e. The emphasis of the dot pattern appears to shift towards the electrode with the lower potential. Existing dots vanish (particularly clear for very large bias; see Fig. 1e) and new dots appear (bottom right of Fig. 1d; bottom left of Fig. 1e) that were not present for low bias. These trends may be due to the effective gate voltage near the right and left electrodes being different at higher bias voltages. Contrast also diminishes when the tube potential approaches the tip voltage.

The electronic properties of semiconducting nanotubes have been proposed to be sensitive to perturbations by local disorder[2,6–8]. Our results confirm the occurrence of such electronic disorder by direct spatial images. The microscopic origin of this disorder is still unclear, however. The most likely causes are localized charges near the nanotube, or mechanical deformations. Detailed height measurements by AFM did not reveal any correlation between height and electronic features.

Our results shed a new light on other reported transport data. Step features have been found in current–voltage (I–V) curves of TUBEFET devices (ref. 3, and S. J. T. *et al.*, unpublished results). Our findings may explain these observations because an increasing bias voltage can bring down the potential barriers one at a time, leading to step-like features. Reported asymmetries in I–V curves[1,3,4] can now be corroborated by the asymmetries in the potential profile along tubes at low bias. In conduction experiments at low temperatures (ref. 8, and Z. Yao *et al.*, unpublished results), phenomena related to multiple metallic islands have been observed, which can be explained by the barrier sequence seen in our SGPI images. Near the tube on top of the electrodes, no contrast could be found in the SGPI images, even for large tip voltages (up to ±3 V). This indicates that Schottky barriers do not exist at the metal interface, as was suggested earlier[4].

New scanning techniques that give a direct view of the potential landscape, such as the one presented here, provide a promising starting point for a better understanding of the electronic structure of nanotube devices. It should, for example, be feasible to study the effect of deliberate bending of nanotubes, different substrate and electrode materials, and the different geometry of devices such as intramolecular kinked-nanotube diodes[5] and nanotube crossings.

Sander J. Tans*†, Cees Dekker*
**Delft University of Technology, Department of*

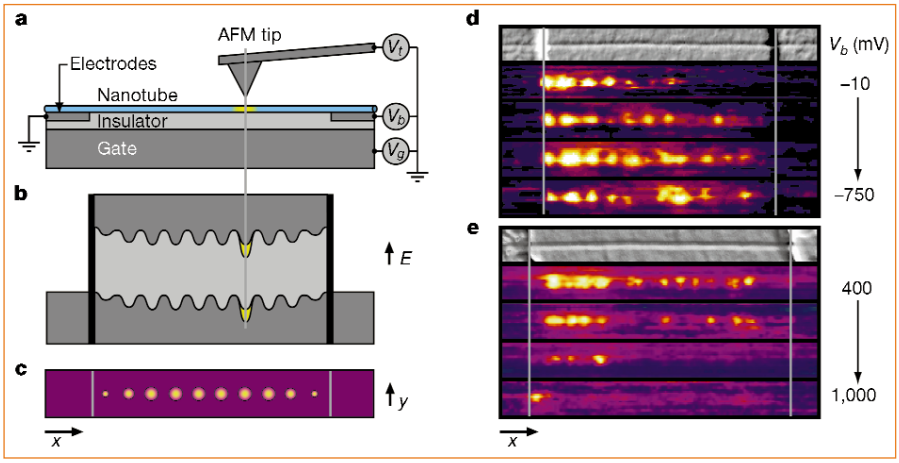

Figure 1 Scanning-gate potential imaging (SGPI) along a semiconducting carbon nanotube. **a,** SGPI measurement set-up. Variable bias voltages, V_b, and a gate voltage, V_g, of −6 V are applied to the TUBEFET device. An atomic-force microscope (AFM) tip at 500 mV is scanned at a constant height of about 10 nm above the surface by retracing each line taken in regular tapping mode AFM while setting a certain height offset and the cantilever amplitude to zero. **b,** Potential landscape of the device. In the conducting state, the valence band edge is horizontal and pinned to the edge of the Fermi level of the electrode[1,9]. The tip voltage creates a potential dip (yellow) which provides a probe for the local potential. SGPI measurements (**d,e**) show that the band edge of the nanotube is not smooth but strongly modulated. **c,** Corresponding SGPI measurement. The device current (colour) is displayed as a function of tip position. Current is reduced when the AFM-tip-induced barrier aligns with minima in the original potential profile. The spatial resolution of the SGPI measurements, which we estimate to be of the order of 10 nm, is determined by the tip–sample distance and the tip radius. **d,** AFM image of the first sample and the corresponding SGPI images for V_b values of −10, −100, −500 and −750 mV (top to bottom). The sample consists of an individual single-wall carbon nanotube (horizontal line) on top of two 25-nm-high platinum electrodes (on the left and right) that are spaced by 650 nm. **e,** AFM image of a second sample and the corresponding SGPI images for V_b values of 400, 500, 700 and 1,000 mV (top to bottom). The sample consists of an individual single-wall carbon nanotube on top of two 750-nm-spaced gold electrodes. The electrodes of this sample are embedded in the SiO_2 substrate to create a flat surface[5] (see **a**).

Applied Physics and DIMES, Lorentzweg 1, 2628 CJ Delft, The Netherlands
†Present address: Department of Physics, University of California, Berkeley, California 94720, USA
e-mail: dekker@qt.tn.tudelft.nl

1. Tans, S . J., Verschueren, R. M. & Dekker, C. *Nature* **393,** 49–52 (1998).
2. Martel, R., Schmidt, T., Shea, H. R., Hertel, T. & Avouris, Ph. *Appl. Phys. Lett.* **73,** 2447–2449 (1998).
3. Antonov, R. D. & Johnson, A. T. *Phys. Rev. Lett.* **83,** 3274–3276 (1999).
4. Soh, H. T. *et al. Appl. Phys. Lett.* **75,** 627–629 (1999).
5. Yao, Z., Postma, H. W. Ch., Balents, L. & Dekker, C. *Nature* **402,** 273–276 (1999).
6. Bezryadin, A., Verschueren, A. R. M., Tans, S. J. & Dekker, C. *Phys. Rev. Lett.* **80,** 4036–4039 (1998).
7. Ando, T. & Nakanishi, T. *Phys. Soc. Jpn* **67,** 1704–1713 (1998).
8. McEuen, P. L., Bockrath, M., Cobden, D. H., Yoon, Y.-G., Louie, S. G. *Phys. Rev. Lett.* **83,** 5098–5101 (1999).
9. Wildoer, J. W. G., Venema, L. C., Rinzler, A. G., Smalley, R. E. & Dekker, C. *Nature* **391,** 59–62 (1998).

Biogeochemistry

Microbial essentials at hydrothermal vents

Hot, anoxic fluids emerging from deep-sea hydrothermal vents mix suddenly with cold oxygenated sea water, providing ideal microbial niches for organisms that need limited amounts of oxygen. We have now identified and grown the first microaerophilic, thermophilic eubacterium from a deep-sea hydrothermal chimney. In view of the likely abundance of this type of microenvironment in hydrothermal structures, these newly discovered thermophilic microbes could constitute a large part of the microbial populations in seafloor hydrothermal systems.

In 1995, using the submersible *DSV Nautile*, we deployed an *in situ* growth chamber on the top of a hydrothermal vent at the Mid-Atlantic Ridge (Snake Pit, 23° 22′ N, 44° 57′ W). After deployment for 5 days (with an *in situ* chamber temperature between 70 and 25 °C), we extracted DNA from samples collected from the chamber. We amplified the genes encoding small-subunit ribosomal RNA (16S rRNA genes)[1] by using the polymerase chain reaction, then cloned and screened them by restriction-fragment length-polymorphism analysis[2].

Representatives of each clone type were completely sequenced (GenBank accession numbers AF068782–AF068824). Phylogenetic analysis revealed that about 13% of the sequences were closely related to *Aquifex*[3] (Fig. 1). These new sequences formed a separate clade from the Aquificales lineage, and grouped most closely with bacterial sequences from terrestrial geothermal springs in Japan[4] and Yellowstone National Park[5,6]; this clade has previously had no representatives in culture.

Environmentally derived 16S rRNA gene sequences may indicate the microbial diversity of an environment, but they tell us little about the physiology and ecology of the organisms themselves. The similarity of our Mid-Atlantic Ridge 16S rRNA sequences to those of the Aquificales persuaded us to try a mixture of hydrogen and oxygen for enriching the population of *Aquifex*-like thermophilic chemolithotrophs (organisms that use inorganic substrates for energy recovery) during a research cruise in 1999 to another hydrothermal vent field at 9° N 104° W. Conservation of physiology over such a phylogenetic depth is unusual among thermophiles, although this is seen in methanogens.

We collected sulphide chimneys from onboard the *DSV Alvin* and ground the samples under an atmosphere of nitrogen. The rock slurry was inoculated into a modified MSH medium (http://caddis.esr.pdx.edu/OCM/) with a headspace containing 1 atmosphere CO_2, 0.05 atmospheres O_2 and 1 atmosphere H_2, and the cultures were incubated at 70 °C. We isolated a highly motile, short rod from one of these enrichment cultures and named it strain EX-H1. Strain EX-H1 grew in the presence of 5% (by volume) O_2, but did not grow well at 10% O_2. The strain also grew anaerobically with nitrate as its sole electron acceptor, like most Aquificales, and did not grow at 95 °C.

We extracted genomic DNA, amplified the 16S rRNA gene and sequenced both strands (GenBank accession no. AF188332). The 16S rDNA sequence was about 78% similar to that of *Aquifex pyrophilus*, and 92% similar to the Mid-Atlantic Ridge deep-sea microbial sequences we obtained in 1995. On the basis of sequence alone, strain EX-H1 can be considered as a member of a new family or order[7], separate from, but most closely related to, the genus *Aquifex*.

To our knowledge, this is the first report of a microaerophilic, hydrogen-gas-oxidizing, chemolithotrophic and thermophilic eubacterium from deep-sea vents. Although this new isolate is only distantly related to *Aquifex*, it shares with the Aquificales the ability to grow under microaerophilic conditions. The steep chemical and oxygen gradients at hydrothermal vents provide ample habitats at low-oxygen tensions that contain reduced substrates such as hydrogen gas. Microaerophiles such as EX-H1 and the archaeum *Pyrolobus fumarii*[8] are therefore uniquely suited to these environments and, like the anaerobic ammonium oxidizers[9], they can put the H_2, CO_2 and small amount of O_2 available at deep-sea hydrothermal vents to good use.

If, based on their much-debated deeply rooted position in the tree of life[9], the Aquificales-like microbes represent living fossils in the bacterial domain, then microaerophily may reflect an ancient metabolic trait. The early Earth had a reducing atmosphere, but small amounts of oxygen may have been available, initially produced photolytically by abiotic reactions and later by oxygenic photosynthesis. These initial low-oxygen conditions provided a selective pressure for the evolution of microbes capable of using oxygen, but without selection for tolerance of the higher oxygen concentrations present in the atmosphere today, thus favouring microaerophile survival. Alternatively[10], the use of oxygen as an electron acceptor may have arisen through lateral gene transfer. The diversity of microbes being discovered must contribute to global biogeochemical cycling.

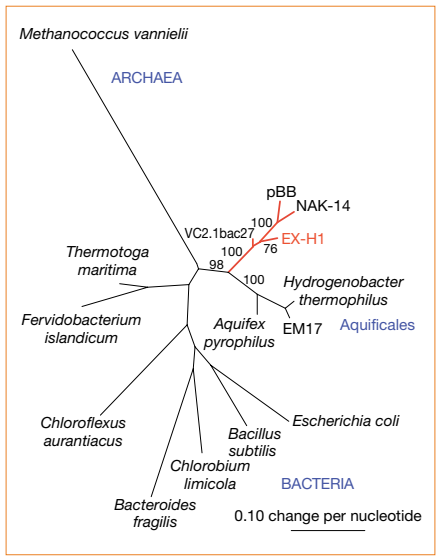

Figure 1 Phylogenetic tree of representatives of the bacterial domain and bacterial 16S rRNA gene sequences obtained from deep-sea (VC2.1bac27), Japan (NAK-14) (ref. 4) and Yellowstone (pBB) (ref. 6) thermal vents. Maximum-likelihood analysis was done using fastDNAml (version 1.1), distributed by the Ribosomal Database Project[11], and the archaeal domain was used as the outgroup. Bootstrap analysis was performed with 100 resampled data sets; only values relevant to EX-H1 are presented.

Anna-Louise Reysenbach*, Amy B. Banta*, David R. Boone*, Stephen C. Cary†, George W. Luther†
**Department of Environmental Biology, Portland State University, Portland, Oregon 97201, USA*
e-mail: ReysenbachA@pdx.edu
†College of Marine Studies, University of Delaware, Lewes, Delaware 19958, USA

1. Ward, D. M., Bateson, M. M., Weller, R. & Ruff-Roberts, A. L. *Adv. Micro. Ecol.* **12,** 219–286 (1992).
2. Reysenbach, A. L., Wickham, G. S. & Pace, N. R. *Appl. Environ. Microbiol.* **60,** 2133–2119 (1994).
3. Aragno, M. in *The Prokaryotes* (eds Barlows, A. *et al.*) 3917–3933 (Springer, New York, 1990).
4. Yamamoto, H. *et al. Appl. Environ. Microbiol.* **64,** 1680–1687 (1998).
5. Hugenholtz, P. *et al. J. Bacteriol.* **180,** 366–376 (1998).
6. Reysenbach, A. L. *et al. Biol. Bull.* **196,** 367–372 (1999).
7. Devereux, R. *et al. J. Bacteriol.* **172,** 3609–3619 (1990).
8. Blochl, E. *et al. Extremophiles* **4,** 14–21 (1997).
9. Strous, M. *et al. Nature* **400,** 446–449 (1999).
10. Doolittle, R. F. *Nature* **392,** 339–342 (1998).
11. Maidak, B. L. *et al. Nucleic Acids Res.* **27,** 171–173 (1999).